materials

MDPI

Communication

Effect of Pore-Forming Agent Type on the Pore Structure and Mechanical and Thermal Properties of Porous Cordierite Ceramics

Da Nie [1,2,*], Hao Wang [1], Yi Li [2], Jianju Wang [2] and Qinghua Chen [1,2,*]

[1] Department of Materials Science and Engineering, Kunming University of Science and Technology, Kunming 650032, China
[2] Yunnan Filter Environmental Protection Technology Co., Ltd., Kunming 650300, China
* Correspondence: ni_eda@163.com (D.N.); chenqinghua_yn1@163.com (Q.C.)

Abstract

Kaolin, talc, silica, boehmite and alumina were used as the main raw materials, and potato starch, corn starch, graphite and PMMA were added as pore-forming agents at an equal volume fraction to prepare porous cordierite ceramics. Experiments were conducted to produce porous cordierite ceramics by incorporating various pore-forming agents at an equal volume ratio. The type of pore-forming agent did not affect the phase composition of the resulting cordierite. The sample prepared with potato starch showed the narrowest pore-size distribution, the best pore interconnectivity, and the lowest coefficient of thermal expansion (0.51×10^{-6} K^{-1}), whereas the PMMA-derived sample had the highest porosity (62.2%) and the graphite-derived sample the highest compressive strength. Considering the properties obtained, the availability of the raw material, and its cost, potato starch is the most suitable pore-forming agent for porous cordierite ceramics. Given the pronounced susceptibility of starch-rich green bodies to drying-induced cracking, future work will focus on hybrid pore-forming systems that partially replace starch with inert pore formers.

Keywords: porous cordierite ceramics; pore-forming agent; median pore size; porosity; coefficient of thermal expansion

1. Introduction

Due to their extremely low thermal expansion coefficients and excellent thermal shock resistance, porous cordierite ceramics are widely used in particulate filters [1–3] and catalyst substrates in automotive exhaust after-treatment systems. Particulate filters can significantly reduce particulate emissions. Figure 1 illustrates the working principle of a wall-flow gasoline particulate filter (GPF). However, enhancing their filtration efficiency by reducing the pore size also increases the pressure drop and fuel consumption. Larger pore sizes in a particle filter result in reduced exhaust resistance but also in decreased particle filtration efficiency. Wu et al. [4] further pointed out that future work should consider vehicle-level performance and fuel economy rather than filter-level metrics alone. However, increased exhaust backpressure can lead to higher fuel consumption. In addition, pore size distribution significantly affects both filtration efficiency and pressure drop in particulate filters. Reducing the pore size and gas flow rate of a particle trap can improve its filtration efficiency. The smaller the filter's average pore size, the higher its efficiency. When the average pore size is less than 12 μm, the pores are prone to being clogged by the catalyst, which leads to a sharp increase in pressure drop. Therefore, researchers believe that an average pore

Check for updates

Academic Editors: Dinesh Agrawal and Zhonghua Yao

Received: 17 October 2026
Revised: 14 November 2026
Accepted: 23 November 2026
Published: 27 November 2026

Copyright: © 2026 by the authors. Licensee MDPI, Basel, Switzerland. This article is an open access article distributed under the terms and conditions of the Creative Commons Attribution (CC BY) license.

size of 12–18 μm is an optimum median pore size. Researchers found that reducing the average pore size from 25 μm to 15 μm increased total filtration efficiency from 80% to 92% [5,6]. Kyoung-Bok Lee et al. [3] investigated the effect of pore size on particulate filter performance and found that as pore size increased from 8.22 to 12.90 μm, pressure drop decreased by 13.60%. In a related study, Boger et al. [7] demonstrated that reducing pore size improves the filtration efficiency of gasoline engine particulate filters. However, this also leads to an increase in backpressure. Additionally, increasing wall thickness enhances filtration efficiency and improves the mechanical strength of the particulate filter but results in a significant increase in backpressure. Boger et al. [7]. investigated how cell density (or mesh size), wall thickness and porosity affect the backpressure of a GPF. As shown in Figure 2, cell density and wall thickness have a more significant impact on GPF backpressure than porosity does. Araji et al. [8] investigated the filtration process of GPF and experimentally verified the impact of various GPF parameters, such as wall thickness, porosity, median pore size (MPS) and length, on filtration efficiency (FE). The results suggested that filtration efficiency increases as soot deposits accumulate, and that median pore size (MPS) has a greater impact on filtration efficiency than wall thickness or filter length. Gong et al. [9] found that the porosity and pore size distribution of GPF carriers significantly influence local particle deposition within the carrier and macroscopic filtration performance. Therefore, it is crucial to develop porous ceramics with high porosity and adjustable pore sizes in order to balance the pressure drop and filtration efficiency of a particulate filter.

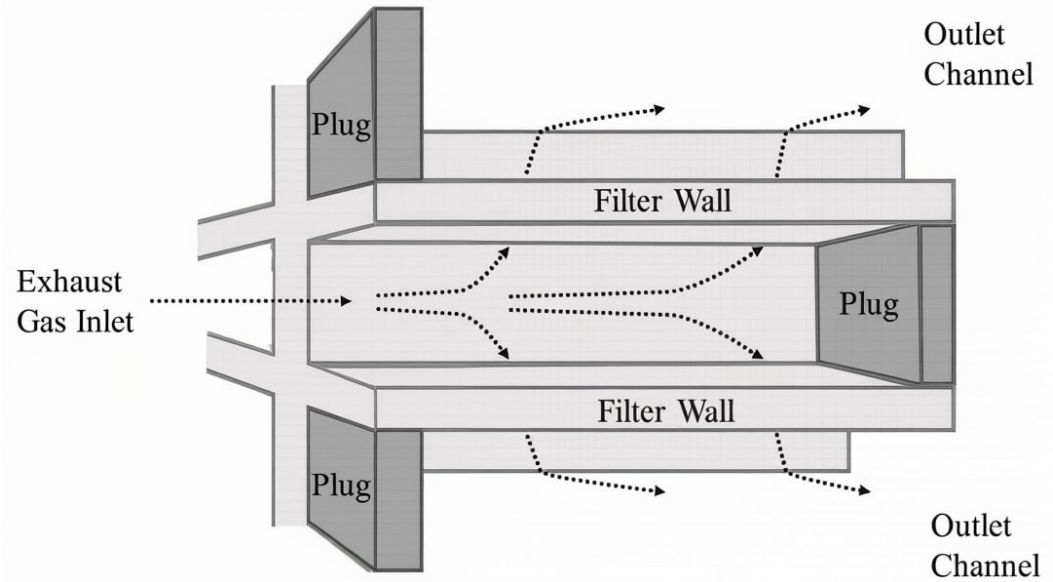


Figure 1. Schematic of the wall-flow filtration principle in a particulate filter (dashed arrows indicate the exhaust gas flow path).

The sacrificial pore-forming agent method is typically used to prepare porous cordierite ceramics. Common pore-forming agents include potato starch, corn starch, graphite, polystyrene (PS) and PMMA. Zhao et al. used graphite [10] as a pore-forming agent to produce porous cordierite ceramics. Their research demonstrated that varying the amount of graphite added could effectively control the porosity, pore size and distribution of porous cordierite materials. The highest porosity was observed in porous cordierite ceramics prepared with 45% graphite. Cheng M. et al. prepared cordierite supports using industrial-grade cordierite powder as the raw material and carbon powder, starch and polystyrene microspheres as pore-forming agents [11]. They reported that cordierite prepared with starch as the pore-forming agent had a higher proportion of closed pores and

poor connectivity. In contrast, cordierite prepared with polystyrene had the highest open porosity as well as the best pore uniformity and connectivity. The starch consolidation method [12] can also be used to prepare porous cordierite ceramics.

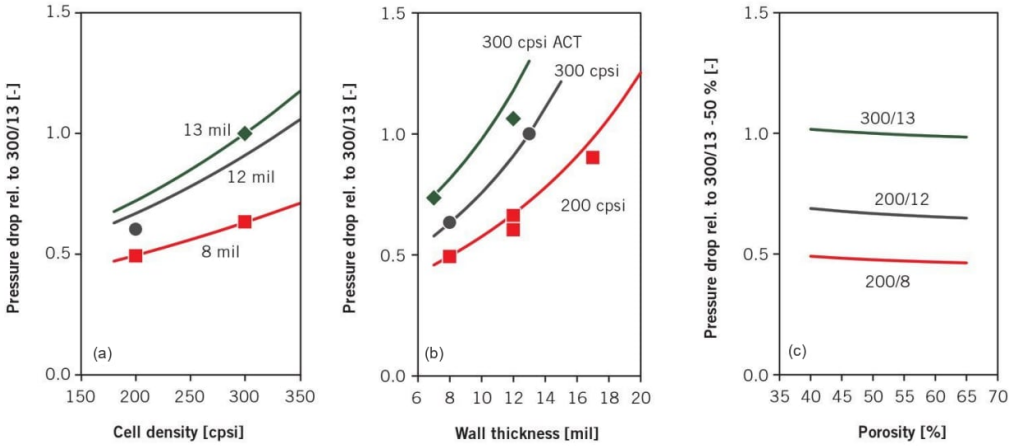


Figure 2. Effect of (**a**) cell density (cpsi), (**b**) wall thickness and (**c**) porosity on back pressure of cordierite particulate filter (without washcoat) [7].

2. Materials and Methods

Potato starch, corn starch, graphite and PMMA were used as pore-forming agents, and talc, kaolin, silica, alumina and boehmite were used as the main raw materials. The main raw material composition was as follows: talc, 39.60 wt%; alumina, 13.86 wt%; silica, 14.85 wt%; calcined kaolin, 3.96 wt%; and washed kaolin, 15.84 wt%. The main raw materials were formulated as follows: talc, 39.60 wt%; alumina, 13.86 wt%; silica, 14.85 wt%; calcined kaolin, 3.96 wt%; and washed kaolin, 15.84 wt%. PVA, PEG, and HPMC were used as binders, with HPMC accounting for 3.96 wt%, and glycerol was added as a moisture-retaining agent at 2.97 wt%. The additions of potato starch, corn starch, PMMA, and graphite were approximately 40, 27.99, 32.7, and 28.7 wt%, respectively, based on the mass of the ceramic powder. Figure 3 shows the particle size distributions of four different pore-forming agents. The pug was processed in a vacuum pug mill and subsequently extruded by a vertical extruder at a forming pressure of 9–10.5 MPa, with a cell density of 400 CPSI and a wall thickness of 0.25 mm. The porous cordierite green bodies were dried in a domestic microwave oven and then sintered in an atmosphere furnace at 1425 °C for 6h. In the experiment, the volume of the pore-forming agent added remained consistent. The amounts of the other pore-forming agents were calculated according to the bulk density, based on the amount of potato starch added. Table 1 shows the particle size, bulk density and masses of the different pore-forming agents, along with the pore size and porosity data for the cordierite porous ceramics made with these agents. The process of preparing porous cordierite ceramics using a pore-forming agent is illustrated in Figure 4.

Particle size distributions of the starting powders were determined by laser diffraction using a Topsizer laser particle size analyzer (Zhuhai OMEC Instruments Co., Ltd., Zhuhai, China). Green bodies were formed by extrusion on a vertical hydraulic extruder (Xiangshan, Ningbo, Zhejiang, China) and sintered in a KSX-30-14 sintering furnace (Wuxi Beirus Thermal Technology Co., Ltd., Wuxi, China). The coefficient of thermal expansion (CTE) was measured with a DIL 402 PC dilatometer (NETZSCH-Gerätebau GmbH, Selb, Germany). Pore size distribution and porosity were characterized by mercury intrusion porosimetry using a PoreMaster 33 porosimeter (Quantachrome Instruments, Anton Paar, Boynton Beach, FL, USA). Compressive strength was measured on an HY-3080 universal testing machine (Shanghai Hengyi Precision Instrument Co., Ltd., Shanghai, China).

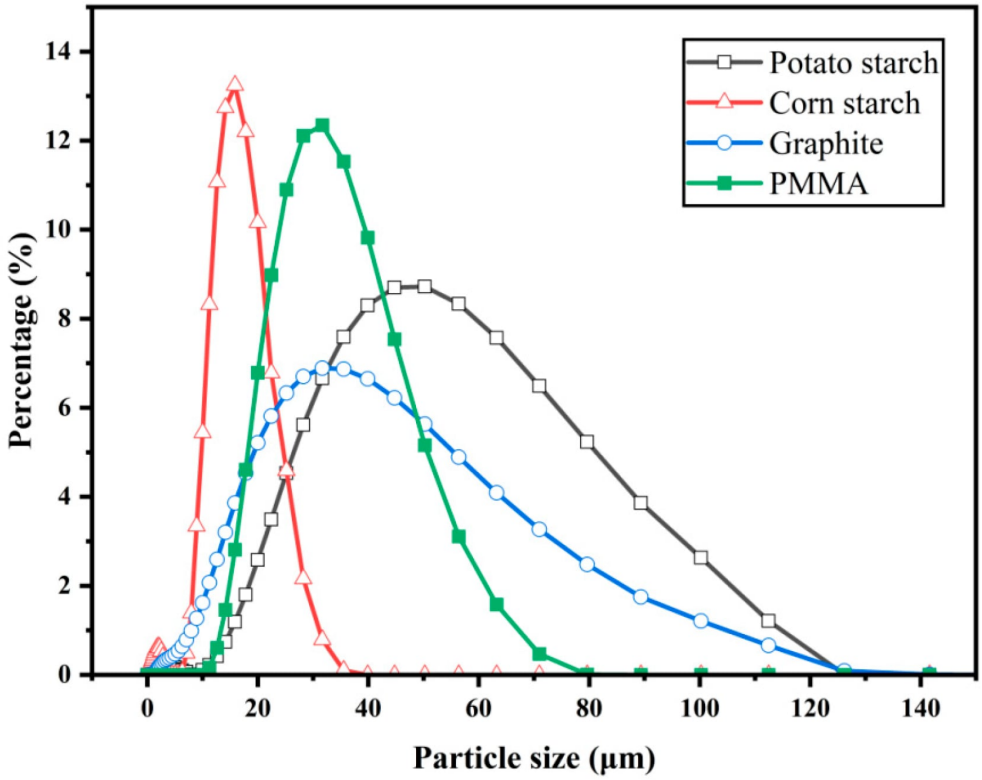


Figure 3. Particle size distributions of the four pore-forming agents.

Table 1. Median particle size, bulk density and added amount of the four pore-forming agents.

Pore-Forming Agent	Median Particle Size/μm	Bulk Density of Pore-Forming Agents/g/cm^3	Mass of Pore-Forming Agent/g
Potato starch	36.77	0.7571	1600.00
Corn starch	14.27	0.5279	1115.63
Graphite	30.30	0.5436	1148.80
PMMA	30.03	0.6197	1309.63

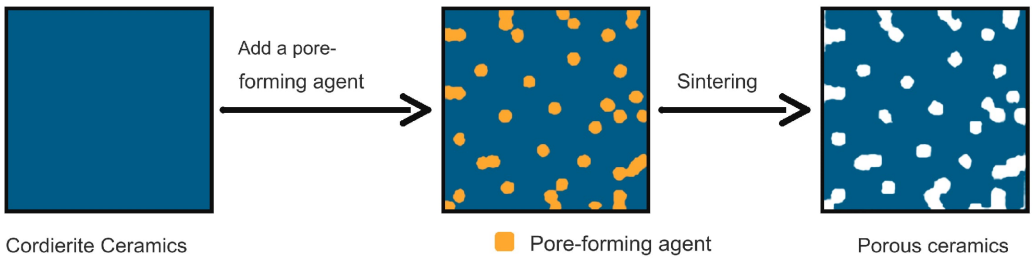


Figure 4. Schematic of the fabrication route for porous cordierite ceramics with a pore-forming agent.

3. Results

3.1. Effect of Pore-Forming Agent Type on the Pore Structure of Porous Cordierite Ceramics

As shown in Figure 5, pore morphology depends strongly on the pore-forming agent. The pore size distribution curves of porous cordierite ceramics prepared using different pore-forming agents are shown in Figure 6. Figure 6 marks the peak pore diameters of the pore size distribution curves for each sample. The data on pore size and porosity for cordierite prepared using different pore-forming agents are summarized in Table 2. Combining Figures 5 and 6 and Table 2 reveals that the corn-starch-derived ceramic had the

smallest median pore size (14.95 μm, mean 17.57 μm). The reason for this is that corn starch has the smallest particle size. The cordierite porous ceramics that were prepared using potato starch as a pore-forming agent had the largest median pore diameter, corresponding to their largest median particle size. The pore size distribution width is calculated by the formula (d90 − d10)/d50, where d90, d50 and d10 are the pore diameters at which the cumulative pore volume reaches 90%, 50% and 10%, respectively; a smaller value indicates a narrower pore size distribution. The cordierite porous ceramics prepared using corn starch had the least-uniform pore-size distribution, whereas those prepared using potato starch had the best. The pore size distribution and median pore size of cordierite porous ceramics prepared using either PMMA or graphite as pore-forming agents are similar. However, cordierite ceramics prepared using PMMA exhibit higher porosity. For a given volume of material, PMMA exhibits the highest pore-forming efficiency, followed by potato starch. Graphite, on the other hand, exhibits the lowest pore formation efficiency.

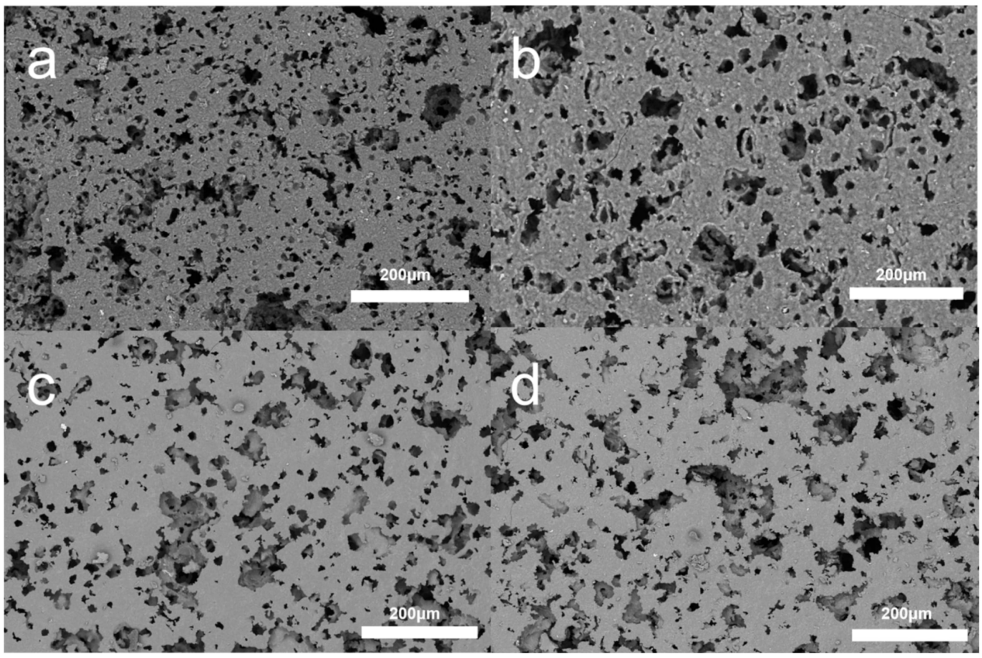


Figure 5. BSE-SEM micrographs of porous cordierite ceramics prepared with (**a**) corn starch, (**b**) potato starch, (**c**) PMMA and (**d**) graphite (500×; scale bars = 200 μm).

Table 2. Pore-structure parameters of porous cordierite ceramics prepared with different pore-forming agents.

Types of Pore-Forming Agents	Open Porosity/%	Specific Pore Volume/$cm^3 \cdot g^{-1}$	Mean Pore Size/μm	Median Pore Size/μm	(d90 − d10)/d50
Without pore-forming agents	37.02	-	-	-	-
Potato starch	60.59	0.63	24.06	22.08	1.17
Corn starch	56.81	0.50	17.57	14.95	1.56
Graphite	40.28	0.35	20.91	18.06	1.23
PMMA	62.23	0.61	20.61	19.32	1.28

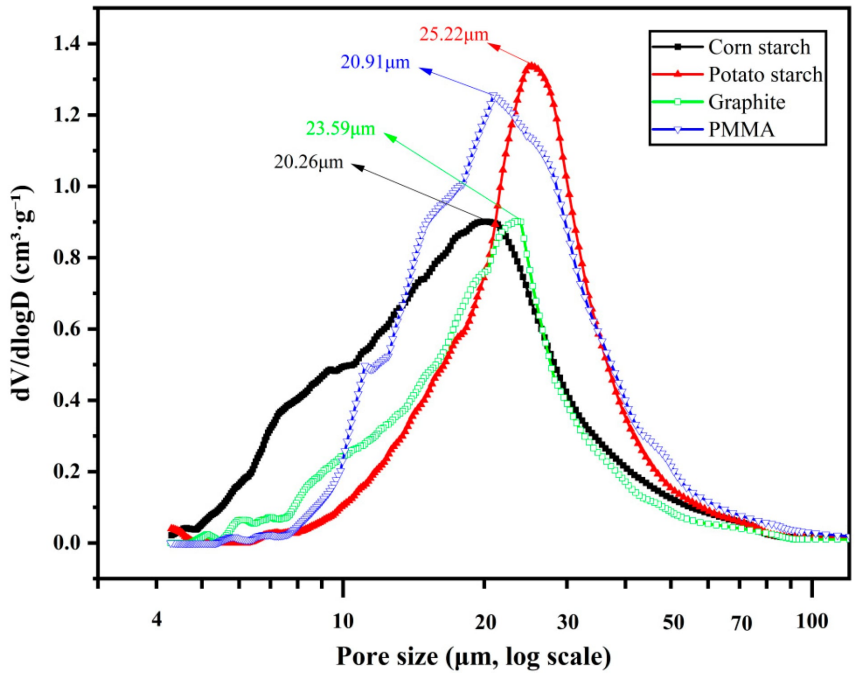


Figure 6. Pore size distribution curves of cordierite porous ceramics prepared using various pore-forming agents.

3.2. The Effect of Different Pore-Forming Agents on the Phase Composition of Cordierite Porous Ceramics

Figure 7 shows the XRD patterns of porous cordierite ceramics prepared with different pore-forming agents. All samples show only the cordierite phase, consistent with PDF# 89-1487, with no detectable secondary phases (within the XRD detection limit, ~3 wt%). This suggests that the different pore-forming agents had no effect on the cordierite main crystal phase. This may be because the pore former is burned out during sintering.

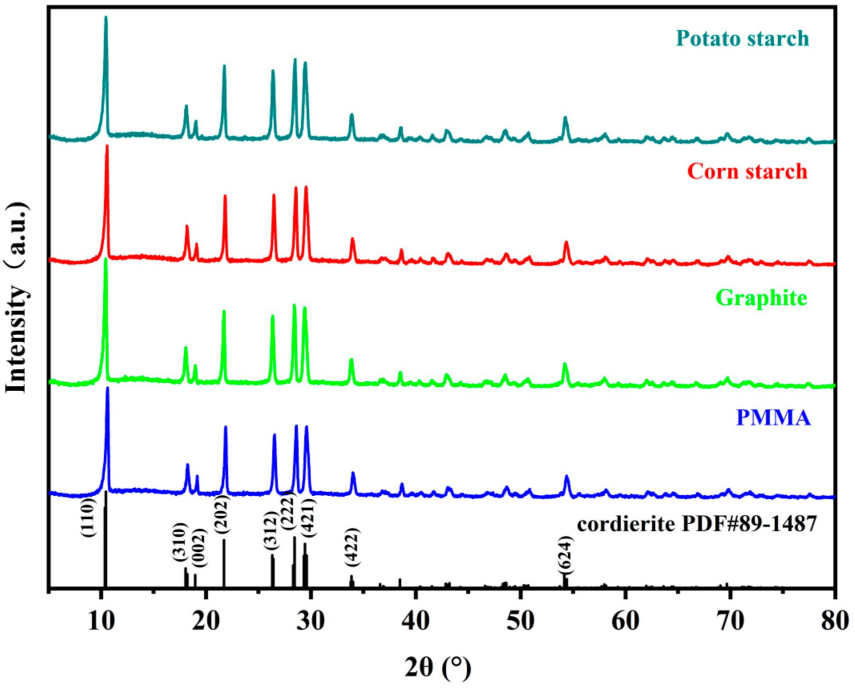


Figure 7. XRD patterns of porous cordierite ceramics prepared using different pore-forming agents.

3.3. Effect of Pore-Forming Agent on the Compressive Strength of Cordierite Porous Ceramics

As shown in Figure 8, the compressive strength along the A-and B-axes of cordierite ceramics prepared using different pore-forming agents is presented. For the compressive strength test standard, refer to GB/T 1964 [13]. The direction along the channels of the honeycomb ceramic is referred to as the A-axis, while the B-axis is perpendicular to this direction. As shown in Figure 8, cordierite porous ceramics prepared using potato starch have the lowest compressive strength (4.49 MPa and 1.13 MPa) along the A and B axes. This is because they have the largest pore size and relatively high porosity. Cordierite porous ceramics prepared using graphite and corn starch exhibit high compressive strength. The two samples exhibited comparable compressive strengths. The reason for this is that their pore sizes are smaller or their porosity is lower [14].

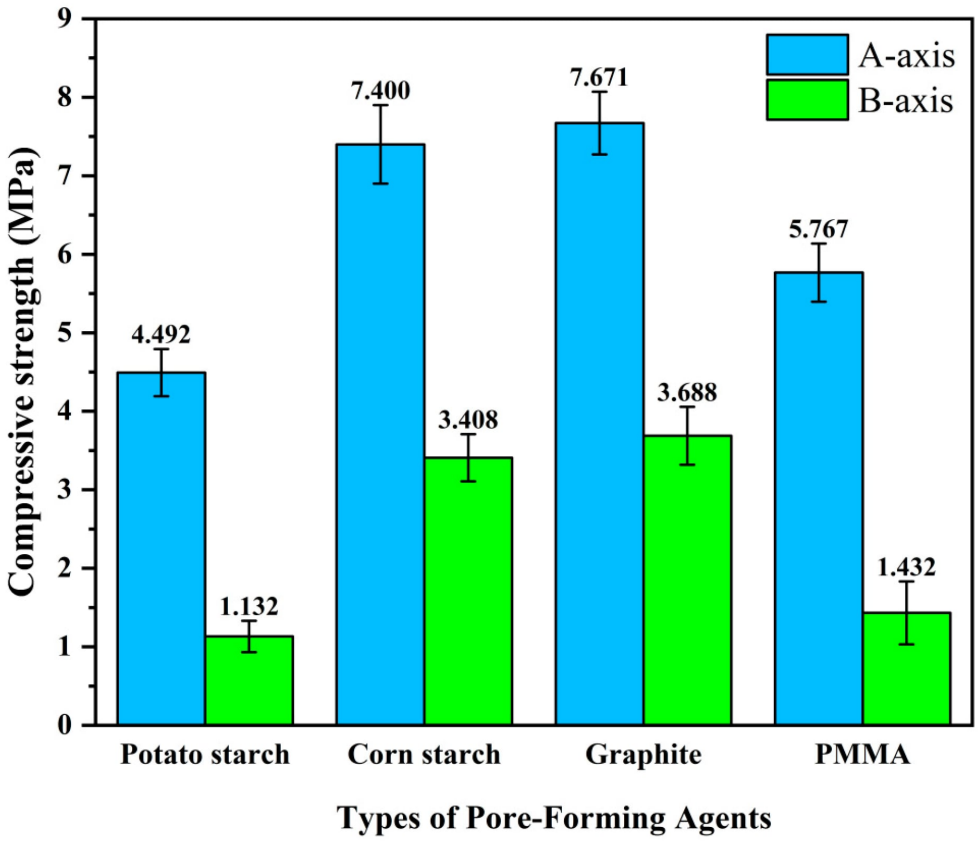


Figure 8. Comparison of the compressive strength of porous cordierite ceramics prepared using different pore-forming agents.

3.4. The Effect of Different Pore-Forming Agents on the Coefficient of Thermal Expansion of Cordierite Porous Ceramics

Figure 9 illustrates the thermal expansion curves of cordierite porous ceramics that were produced using four distinct pore-forming agents at temperatures between 30 and 800 °C. Cordierite ceramics prepared using potato starch as a pore-forming agent have the lowest coefficient of thermal expansion, with an approximate value of $0.51 \times 10^{-6}K^{-1}$. This is because cordierite ceramics prepared using potato starch as a pore-forming agent have the largest pore size and higher porosity, and high porosity lowers the elastic modulus and accommodates thermal strain, thereby reducing the thermal stress during heating. Cordierite ceramics prepared with corn starch and graphite as pore-forming agents have the highest coefficients of thermal expansion, approximately 0.80×10^{-6} and $0.82 \times 10^{-6}K^{-1}$, respectively. The CTE of cordierite ceramics prepared using corn starch as a pore-forming

agent is relatively high due to their small pore sizes and broad pore size distribution. Although cordierite ceramics prepared using graphite as a pore-forming agent exhibit relatively large pore sizes and good pore size distribution, their low porosity results in a relatively high CTE. Additionally, the graphite residue remaining after burning at 1050 °C is approximately 0.20–0.30wt%. The residue from graphite combustion is another factor contributing to its high CTE.

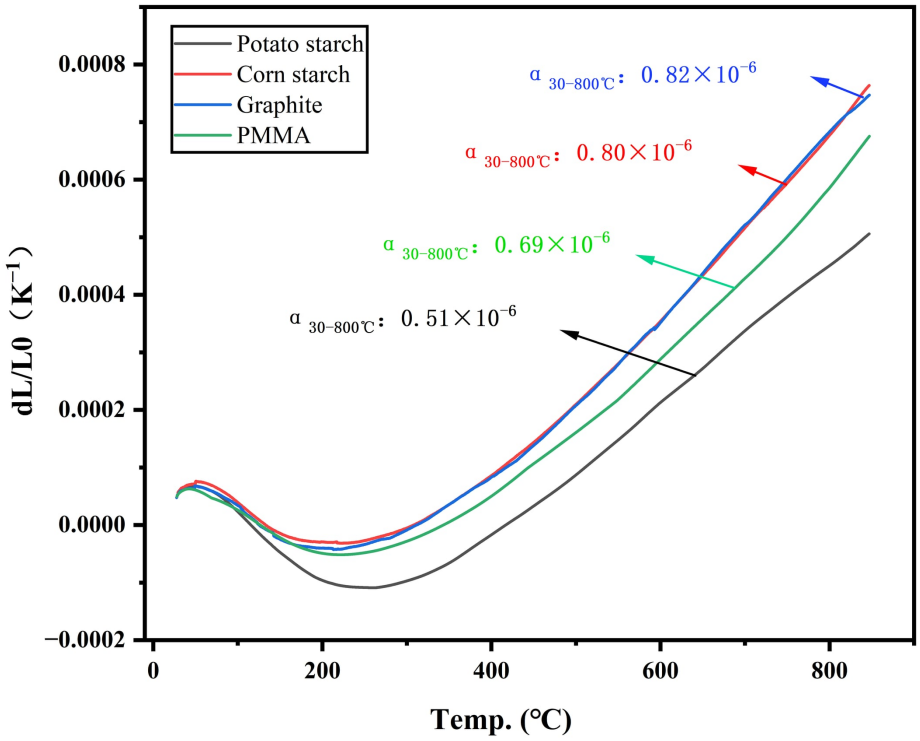


Figure 9. The thermal expansion curves of porous cordierite ceramics that were prepared using different pore-forming agents thermal expansion curves.

4. Discussion

The above test results show that, since the pore-forming agent is decomposed and removed during sintering, using different pore-forming agents has no effect on the phase composition of the cordierite. Among the four pore-forming agents tested, potato starch performed best overall in the preparation of porous cordierite ceramics in terms of median pore size, pore size distribution, coefficient of thermal expansion, compressive strength, and porosity. Cordierite prepared using as a pore-forming agent has the largest pore size and the best pore size distribution. It also has the lowest coefficient of thermal expansion and relatively high porosity. Although cordierite ceramics prepared using corn starch as a pore-forming agent have relatively high porosity, their pore sizes are small, and their pore size distribution is poor. This may be related to the small particle size of the corn starch itself. Ceramics made from cordierite using PMMA as a pore-forming agent exhibit the highest porosity, which indicates that PMMA is a highly effective pore-forming agent. Although the particle size of PMMA can be controlled relatively easily as it is a synthetic material, its high cost limits its use. At the same volume, cordierite prepared with graphite as the pore-forming agent has the lowest porosity. Although graphite was the least effective pore-forming agent, its high burnout temperature and good thermal conductivity make it highly beneficial for ceramic sintering. In addition, adding a high proportion of potato starch to the ceramic green body has been shown to cause cracking during the drying process.

5. Conclusions

Based on the measured properties and a cost comparison, potato starch is the most suitable single pore-forming agent for porous cordierite ceramics. The median pore diameter of the porous cordierite ceramics prepared using potato starch as a pore-forming agent is approximately 22.08 μm, and the porosity is around 60.59%. With a pore size distribution index of approximately 1.17, potato starch is a material well-suited for use as a pore-forming agent in GPF, indicating a uniform pore structure that is favourable for gas flow and pressure drop control. Starch is strongly hydrophilic, readily swells and gelatinizes in aqueous media, and possesses a comparatively coarse granule size; at high loading levels, the green bodies are therefore highly susceptible to drying-induced cracking. Using a composite pore-forming agent could combine the advantages of different pore-forming agents. The development of composite pore-forming systems, in which starch is partially replaced by inert pore formers, thus represents a key direction for future work.

Author Contributions: Conceptualization, D.N. and Y.L.; investigation, H.W. and J.W.; resources, Y.L.; data curation, D.N., H.W. and J.W.; writing—original draft preparation, D.N. and Q.C.; visualization, D.N. and H.W.; supervision, Q.C.; project administration, D.N.; funding acquisition, Y.L. All authors have read and agreed to the published version of the manuscript.

Funding: This work was financially supported by the Yunnan Provincial International Joint R&D Centre for Clean Internal Combustion Engine Emission Technology (202303AP140016), a program of the Yunnan Provincial Science and Technology Program.

Institutional Review Board Statement: Not applicable.

Informed Consent Statement: Not applicable.

Data Availability Statement: The original contributions presented in this study are included in the article. Further inquiries can be directed to the corresponding authors.

Conflicts of Interest: Authors Da Nie, Yi Li, Jianju Wang and Qinghua Chen were employed by the Yunnan Filter Environmental Protection Technology Co., Ltd. The remaining author declares no conflicts of interest.

Abbreviations

The following abbreviations are used in this manuscript:

GPF	Gasoline particulate filter
FE	Filtration efficiency
PS	Polystyrene
PMMA	Poly methyl meth acrylate
CTE	Coefficient of thermal expansion
SEM	Scanning electron microscope
BSE	Back scattered electron
MPS	Median pore size

References

1. Outland, R.J. Ceramic Filters for Diesel Exhaust Particulates. U.S. Patent 4,276,071, 30 June 1981.
2. Wang, Z.; Liu, P.; Li, H.; Li, R.; Pan, X.; Zhao, Y. The Development of Diesel Particulate Filter Technology. *IOP Conf. Ser. Earth Environ. Sci.* **2021**, *632*, 032012. [CrossRef]
3. Lee, K.B.; Kim, S.H.; Oh, K.C. The Effect of Pore Structure on Thermal Characteristics of a Cordierite Diesel Particulate Filter for Heavy Duty Diesel Vehicle. *Int. J. Automot. Technol.* **2021**, *22*, 243–251. [CrossRef]
4. Wu, F.; Jiang, F.; Meng, M. Gasoline Particulate Filter Technology for CHINA Stage-6 Emission Legislation. In *Proceedings of SAE-China Congress 2015: Selected Papers*; Lecture Notes in Electrical Engineering; Springer: Singapore, 2016; Volume 364, pp. 109–115. [CrossRef]

5. Ohara, E.; Mizuno, Y.; Miyairi, Y.; Mizutani, T.; Yuuki, K.; Noguchi, Y.; Hiramatsu, T.; Makino, M.; Takahashi, A.; Sakai, H.; et al. *Filtration Behavior of Diesel Particulate Filters (1)*; SAE Technical Paper 2007-01-0921; SAE International: Warrendale, PA, USA, 2007. [CrossRef]
6. Mizutani, T.; Kaneda, A.; Ichikawa, S.; Miyairi, Y.; Ohara, E.; Takahashi, A.; Yuuki, K.; Matsuda, H.; Kurachi, H.; Toyoshima, T.; et al. *Filtration Behavior of Diesel Particulate Filters (2)*; SAE Technical Paper 2007-01-0923; SAE International: Warrendale, PA, USA, 2007. [CrossRef]
7. Boger, T.; Gunasekaran, N.; Bhargava, R.; Bischof, C. Particulate Filters for DI Gasoline Engines. *MTZ Worldw.* **2013**, *74*, 12–17. [CrossRef]
8. Araji, F.; Matida, E.; Huang, X. *Effects of Porosity, Wall Thickness, and Length on the Filtration Efficiency of Gasoline Particulate Filters*; SAE Technical Paper 2022-01-5010; SAE International: Warrendale, PA, USA, 2022. [CrossRef]
9. Gong, J.; Stewart, M.L.; Zelenyuk, A.; Strzelec, A.; Viswanathan, S.; Rothamer, D.A.; Foster, D.E.; Rutland, C.J. Importance of Filter's Microstructure in Dynamic Filtration Modeling of Gasoline Particulate Filters (GPFs): Inhomogeneous Porosity and Pore Size Distribution. *Chem. Eng. J.* **2018**, *338*, 15–26. [CrossRef]
10. Zhao, G.; Bai, Y.; Qiao, L.; Huang, F. Preparation of Porous Cordierite Ceramics Using Graphite as Pore-Forming Agent. *Refractories* **2014**, *48*, 278–281. (In Chinese) [CrossRef]
11. Cheng, M.; Tian, M.K.; Tao, W.L.; Li, L.J.; Yan, T.G.; Yuan, Y.T. Effect of Pore-Forming Agent and Sintering Temperature on Properties of Cordierite Support. *J. Synth. Cryst.* **2018**, *47*, 2515–2521. (In Chinese)
12. Sandoval, M.L.; Talou, M.H.; Tomba Martinez, A.G.; Camerucci, M.A.; Gregorová, E.; Pabst, W. Porous Cordierite-Based Ceramics Processed by Starch Consolidation Casting—Microstructure and High-Temperature Mechanical Behavior. *Ceram. Int.* **2018**, *44*, 3893–3903. [CrossRef]
13. *GB/T 1964—1996*; Test Method for Crushing Strength of Porous Ceramic. Standards Press of China: Beijing, China, 1996.
14. Ohji, T.; Fukushima, M. Macro-porous ceramics: Processing and properties. *Int. Mater. Rev.* **2012**, *57*, 115–131. [CrossRef]

Disclaimer/Publisher's Note: The statements, opinions and data contained in all publications are solely those of the individual author(s) and contributor(s) and not of MDPI and/or the editor(s). MDPI and/or the editor(s) disclaim responsibility for any injury to people or property resulting from any ideas, methods, instructions or products referred to in the content.